

PERFORMANCE EVALUATION OF GNSS/VISUAL ODOMETRY-BASED POSITIONING AND RANGING SYSTEMS ON UAVS FOR INFRASTRUCTURE INSPECTION

Kazuha Saito¹, Masafumi Nakagawa² and Yusuke Kawasaki³, Masaaki Takebayashi⁴,
Hirotohi Kurashige⁵, Shozo Nishimura⁶, Masafumi Miwa⁷

^{1,2} Shibaura Institute of Technology, 3-7-5 Toyosu, Koto-ku, Tokyo, 135-8548, Japan

^{3,4,5,6} Keisoku Research Consultant CO., 1665-1 Fukuda, Higashi-ku, Hiroshima-shi, Hiroshima, 732-0029, Japan

⁷ Tokushima University, 2-1 Minamijousanjima-cho, Tokushima, 770-8506, Japan

Email: ah18037@shibaura-it.ac.jp; mnaka@shibaura-it.ac.jp

KEY WORDS: UAV; GNSS; Visual odometry; IMU Stereo camera; Indoor-outdoor seamless positioning

ABSTRACT: Unmanned aerial vehicles (UAVs) for infrastructure inspection are required positioning and ranging functions to prevent collisions with structures in poor global navigation satellite system (GNSS) positioning environments, such as spaces under bridges. However, if real time kinematic (RTK) -GNSS positioning is suddenly interrupted, it is necessary to switch to indoor positioning, so these functions alone are not sufficient for stable UAV flights. Thus, indoor/outdoor seamless positioning systems are required for UAVs. Indoor/outdoor seamless positioning systems on UAVs must be compact, lightweight, low-power, low-cost, weather-resistant, and independent of the communication environment. Therefore, we will focus on visual odometry processing to meet these needs. In this study, we propose a methodology to integrate RTK-GNSS positioning and visual odometry using RealSense T265 (Intel) as an inertial measurement unit (IMU) stereo camera with real-time correction of accumulated errors for UAV flights in indoor and outdoor environments. First, a walking measurement experiment was conducted to evaluate the accuracy of ranging systems using IMU stereo cameras and the performance of accumulated error adjustment. We then conducted a flight experiment to verify our methodology under a bridge using a UAV.

1. INTRODUCTION

Recently, UAVs for infrastructure inspections have been equipped with GNSS positioning devices and distance measurement sensors to avoid collisions with objects and structures such as bridges, dams, and towers. Conventional UAVs are mainly controlled with GNSS positioning devices in outdoor environments. Stable flight is achieved with GNSS positioning. However, a poor GNSS environment exists around structures because GNSS positioning is subject to multipath problems around infrastructures. A poor GNSS environment exists around structures. Thus, indoor/outdoor seamless positioning systems are required for UAVs (Mostafa et al., 2018). Therefore, we focus on visual odometry processing (Davide et al., 2011) as an indoor/outdoor seamless positioning system to support the availability of a GNSS positioning environment. Visual odometry is a part of SLAM processing (Faragher et al., 2013; Bassiri et al., 2018), and SLAM processing can be roughly separated into LiDAR SLAM and visual SLAM. Visual SLAM with a single camera has the advantages of inexpensive and light weight. However, SLAM also includes processing costs. Moreover, the accuracy and quality of processing results depend on the environment. In conventional studies, a stereo camera or a combination of a single camera and an IMU is used for visual SLAM to improve the accuracy of position and orientation estimation in visual odometry (Taragay et al., 2007; Yunliang et al., 2013). Thus, we focus on the performance improvement of visual odometry and visual SLAM with multidirectional image acquisition with multi-stereo cameras equipped with an IMU (IMU stereo camera) (Peidong et al., 2018). We also use IMU stereo cameras as depth sensors for ranging systems for obstacle detection and avoidance for autonomous control of UAVs. First, we propose a methodology to detect loop closures in visual odometry to improve the redundancy of camera position and orientation estimation with accumulated error adjustment. Next, we provide an overview of our experiments. In the walking measurement experiment, we verify the accuracy of distance estimation by disparity calculation in indoor and outdoor environments. Then, we summarize and discuss our acquired data and experimental results. We also verify whether our methodology can compensate for cumulative errors by improving the relocalization process in visual odometry. Moreover, we verify that our methodology can provide smooth flight paths in indoor and outdoor environments in UAV flight experiments. We also verify using visual odometry whether the positioning accuracy indoors depends on the camera direction and time variation of the image sequence. Finally, we provide an overview of our experiment.

2. METHODOLOGY

Figure 1 shows our methodology proposed in this study. The proposed indoor/outdoor seamless positioning methodology (GNSS/visual odometry) is a combination of outdoor positioning with GNSS and indoor positioning with visual odometry processing for position and orientation estimation. First, after RTK-GNSS positioning is started, the positioning mode is determined and controlled with confirmed RTK-GNSS positioning status, such as RTK-Fix, RTK-Float, single positioning, and no signals, to obtain the position, rotation, and azimuth data from IMU stereo cameras and the RTK-GNSS receiver. Next, when the RTK-GNSS positioning status = Fix, position data are received from the RTK-GNSS receiver system, which transforms the coordinates. When the RTK-GNSS positioning status = Float, we acquire position, speed, and azimuth data of visual odometry with the IMU stereo cameras. We also generate the rotation and translation using the position data from which the last status = Fix is acquired when we move from outdoor to indoor environments as the origin, and then apply the visual odometry results. Then, we regenerate the NMEA data from the position, velocity, and azimuth data by correcting the applied results with the adjustment control of accumulation error. In the adjustment control of accumulation error in indoor positioning, when a loop closing is detected with local camera translation values among scenes, the error value of camera position and orientation is determined by the difference between a start and goal position when a loop closure is detected with local camera translation values. Moreover, camera position and orientation are relocalized as a landmark update process. Then, control sections are grouped into each section using relocalized positions, and readjusted error values are determined with linear interpolation. In UAV flight operations, the proposed methodology is applied for indoor/outdoor seamless positioning with RTK-GNSS positioning and visual odometry data. The positioning mode such as GNSS positioning and visual odometry is determined by the RTK-GNSS positioning status. Based on these processes, UAVs can receive NMEA data continuously even if there are no GNSS signals to achieve UAV flights in indoor spaces.

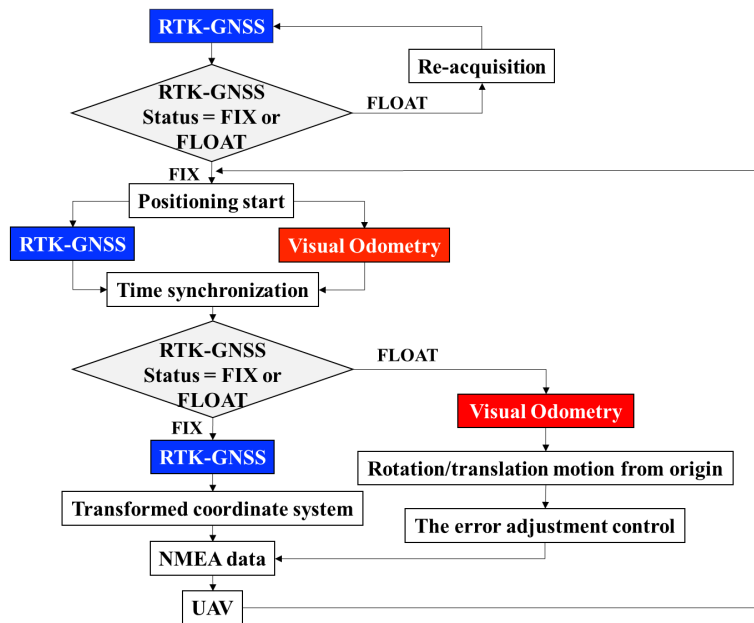


Figure 1. Proposed methodology

2.1 Visual odometry

Visual odometry consists of camera position and orientation estimation processing as a part of visual SLAM processing. In conventional studies, a stereo camera or IMU stereo camera is used to improve the position and orientation accuracy of visual odometry. In this study, we examine a methodology using IMU stereo cameras in multiple directions.

2.2 Positioning mode-changing with multifrequency RTK-GNSS

In this study, we control the positioning modes with RTK-GNSS positioning status, such as RTK-Fix, RTK-Float, and no GNSS signals. When a rover moves from outdoor to indoor space, the position and orientation are first determined by RTK-GNSS positioning with RTK-Fix status. Then, the RTK-Fix status is changed into RTK-Float status in indoor space. During the status change, visual odometry is the initialized position and orientation using GNSS positioning results, and positioning is continued with visual odometry. When a rover moves from indoor to outdoor space, visual odometry is continued by the timing of RTK-Fix status acquisition. When the status changes from RTK-Float to RTK-Fix, the position and orientation are determined by RTK-GNSS positioning.

2.3 Adjustment control of accumulation error

Error accumulation is among the technical issues related to visual odometry and SLAM, as shown in Figure 2. Generally, the accumulation errors are rectified with loop closures. First, a relocalized position is detected as a loop-closed point. Next, the detected position is used to estimate the error adjustment value. Finally, the accumulation error is gradually corrected after relocalization processing. However, error correction is not suitable for real-time processing of UAV flights, because sudden changes make a UAV flight operation unstable. Therefore, we detect the timing of loop closing estimated by an IMU stereo camera to avoid sudden changes in camera position estimation. We also rectify estimated errors gradually to avoid sudden position and orientation changes in a UAV flight operation.

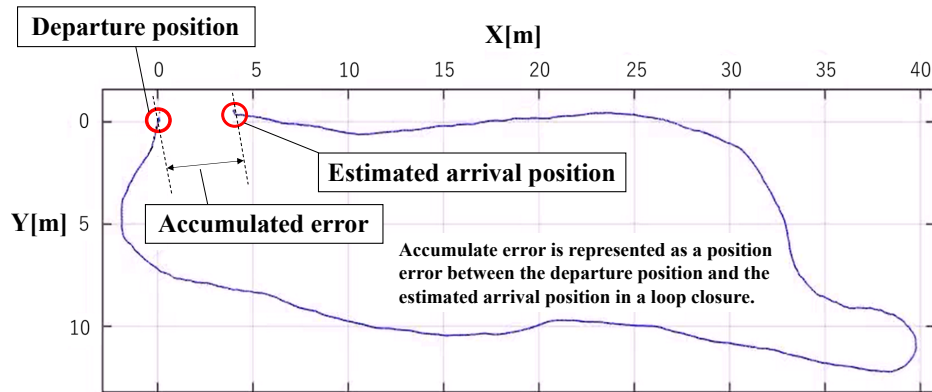


Figure 2. Example of error accumulation

3. EXPERIMENTS

3.1 Walking measurement experiment

In this study, we conducted two types of experiments using IMU stereo cameras (RealSense T265, Intel). First, we conducted the walking measurement experiment on camera position and orientation estimation with movement along a study path to verify the accuracy of visual odometry using the IMU stereo camera in a real space (Figure 3). We selected a path through the indoor and outdoor environments to confirm how the camera images of the indoor environment changed using Door 1 and Door 2. The RTK-GNSS receiver and antenna were ZED-F9P (u-blox) and GNSS antennas, as shown in Figure 4. We also equipped the rover with three IMU stereo cameras (front, left, and top) to cover three directions, as shown in Figure 5. We selected RealSense T265 (Intel) (Table 1) as an IMU stereo camera. All cameras were synchronized with 0.005 (sec) accuracy.

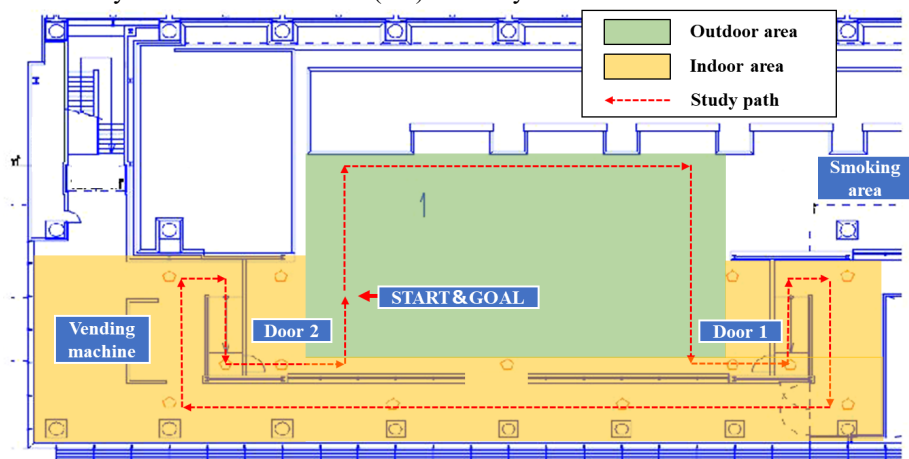


Figure 3. Study path

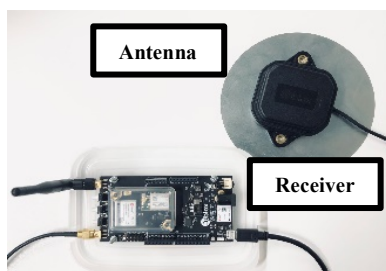


Figure 4. RTK-GNSS receiver and antenna

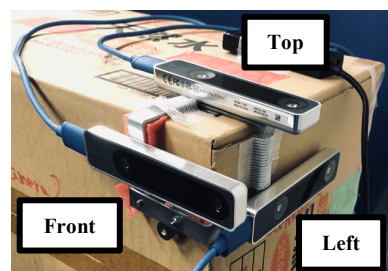


Figure 5. IMU stereo cameras

3.2 UAV flight experiment

We conducted flight experiments to evaluate our methodology for UAV control under bridges (Figure 6) with the indoor/outdoor seamless flight system proposed in this study. IMU stereo cameras (RealSense T265, Intel) in six directions were mounted on a UAV with an RTK-GNSS antenna and receiver (mosaic-X5, Septentrio). We acquired data at 1 (Hz) for GNSS positioning and 10 (Hz) for visual odometry.

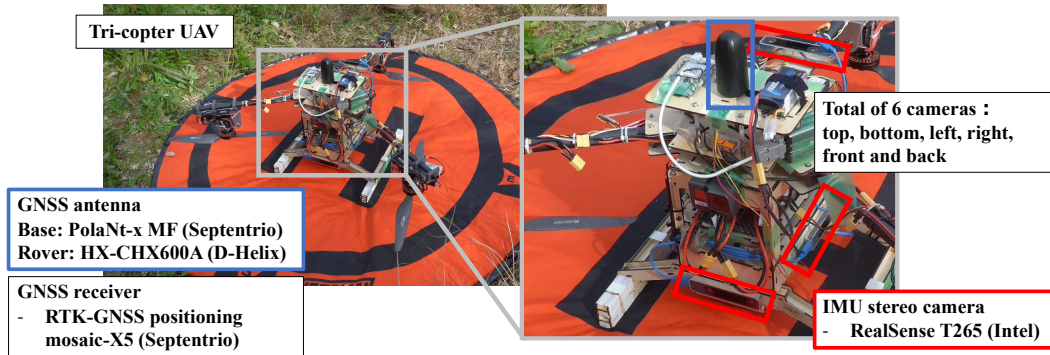


Figure 6. Tricopter UAV

4. RESULTS

4.1 Walking measurement experiment results

The trajectory data and correction data output from the RTK-GNSS positioning and camera position and orientation estimation (front, left, and top) in the walking measurement experiment are shown in Figure 7. The red line indicates RTK-GNSS, the blue dots indicate the estimated visual odometry, the blue circle indicates the start and the red square indicates the goal. In the camera position and attitude estimation, camera position estimation errors occur because of the small number of feature points extracted from the image, resulting in a difference between the actual and estimated paths.

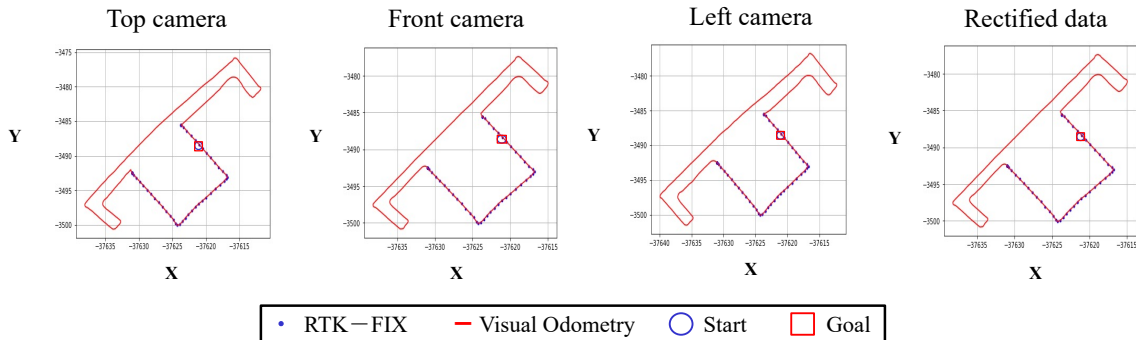


Figure 7. Comparison of trajectory data (each camera)

4.2 UAV flight experiment results

Figure 8 shows the trajectory data estimated in the UAV flight experiment. We confirmed that our methodology can provide smooth flight paths in indoor and outdoor environments. We also confirmed that IMU stereo cameras can support non-GNSS positioning sections when the RTK-GNSS positioning status was less accurate than the Float solution. In UAV flight experiments, we acquired 3293 RTK-GNSS points.

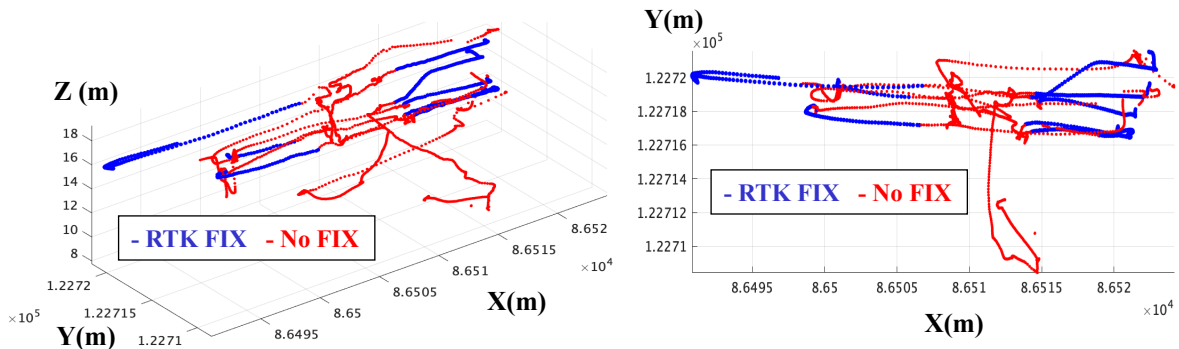


Figure 8. UAV trajectory data(Left image: 3D plot, right image: 2D plot)

5. DISCUSSION

We compared the temporal changes at each frame in the camera position estimation of the acquired and corrected data as shown in Figure 9. In the results of the top camera, the sharp position change was observed at 52 (sec) and was assumed to be relocalized points. We also confirmed that the temporal changes at each frame increased because of the sampling rate difference between RTK-GNSS positioning and visual odometry, when the positioning mode switches from indoor space to outdoor space. Therefore, we confirmed that loop closure was caused by incorrect tracking because of a significant reduction in the number of correspondence points tracked from the feature checkout. The red dots indicate the locations where loop closure occurred. We confirmed that the temporal changes at each frame can be compensated by stepwise correction at the loop closure point using the results of camera position estimation in the other directions (front, left). In addition, we confirmed that the image acquisition in the outdoor environment was set to the RTK-GNSS sampling rate of 10 (Hz), and that the relative position was acquired by position and orientation estimation of visual odometry when the absolute position of RTK-GNSS (status = Fix) was observed. Therefore, we indicated that the sampling rate of visual odometry was reduced to 1 (Hz). As a result, in indoor and outdoor environments, UAVs can be controlled with the RTK-GNSS sampling rate from 5 to 10(Hz). In this study, we note that the sampling rate of indoor/outdoor seamless positioning should be adjusted to visual odometry to conduct feature point detection by camera position estimation.

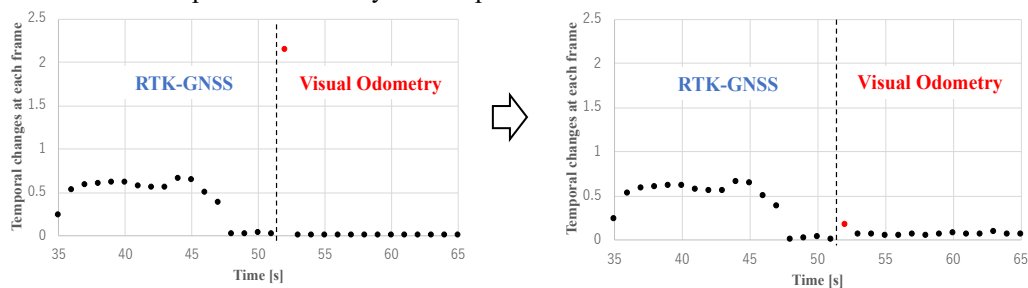


Figure 9. Temporal changes at each frame in camera position estimation

(Left graph: readjusted data without the proposed methodology,
right graph: readjusted data with the proposed methodology)

In this study, we used IMU stereo cameras as depth sensors for ranging systems for obstacle detection and avoidance for autonomous control of UAVs. We confirmed that the minimum range of distance estimation is 0.1 (m) and the maximum is 1.5 (m). We also tracked the corresponding points from the stereo images and acquired the distances of the objects in the field of view. We used the OpenCV library to calculate the disparity in the stereo image. We also implemented an alert function when the distance of the camera to objects was less than 0.3 (m). The quantity of disparity calculation is reduced by limiting the range of disparity calculation and this reduces the complexity of the process. We increased the distance accuracy by increasing the number of pixels in the camera image by maximizing the viewing angle of the stereo camera. As a result, we confirmed that the distance estimation accuracy of ranging systems was approximately 0.1 (m) in indoor and outdoor environments.



Figure 10. Ranging systems for obstacle detection and avoidance

(Left image: disparity image, right image: processed areas in stereo camera image)

We confirmed that the use of visual odometry depends on the number of errors of closure (Table 1). The camera directions and distances from a camera to objects are related to scene changes in sequenced camera images. Thus, rapid turns and image acquisition from closed points affects the accuracy of visual odometry. The error of closure in the walking measurement experiment was respectively 0.03 (m) (front camera), 0.59 (m) (left camera), and 2.77 (m) (top camera). Compared with the front camera, the left camera and the top camera captured more sky and window glass, making it difficult to detect feature points. In this case, we set the front camera to be the camera in the movement direction, which resulted in the smallest error in the closed position. Thus, we note that the camera direction is one of the factors in measurement accuracy improvement in position estimation.

Table 1. Error of closure and ratio of closure

	Error of closure	Ratio of closure
Front camera	0.03 (m)	1/3333
Left camera	0.59 (m)	1/181
Top camera	2.77 (m)	1/38

In UAV flight experiments, we confirmed that a relationship exists between the RTK-Fix rate and error accumulation correction. We also confirmed that the error accumulation increased with the measurement time in visual odometry. Moreover, we confirmed that multifrequency RTK-GNSS positioning improved the speed of refixing. In our preliminary experiment on single-frequency RTK-GNSS positioning, we confirmed that the low refix speed was a technical issue in indoor/outdoor seamless positioning. We confirmed that this issue increases the accumulated error because of the increased position and orientation estimation time of visual odometry. Multifrequency RTK-GNSS positioning can solve the technical issue of a low refix speed by reducing the refix time. Thus, a faster refix in RTK-GNSS positioning can achieve more stable indoor/outdoor seamless positioning. Therefore, we confirmed that RTK-GNSS positioning is effective for indoor and outdoor positioning. In this study, we focused on the performance improvement of visual odometry with multidirectional image acquisition using IMU stereo cameras. We confirmed that the position and orientation estimation using the camera following the flight direction represented the most similar trajectory to that of the actual trajectory. On the other hand, position and orientation estimation often failed when the camera orthogonal to the flight direction was used. Thus, the main camera selection must adapt to flight directions to improve the visual odometry performance of the UAV flight. Our future works are described as follows. First, although high-resolution images can be captured from UAVs with our proposed positioning methodology in infrastructure inspection work, obtained image management is required for change detection and 3D modeling of infrastructures. Thus, we will develop a methodology to manage high-resolution images obtained using UAVs in geographical information systems and building information modeling software products. UAVs are also required ranging systems for obstacle detection and avoidance for autonomous control in infrastructure inspection works. Thus, we will use IMU stereo cameras for visual odometry as depth sensors.

6. CONCLUSION

We proposed a methodology to integrate RTK-GNSS positioning and visual odometry with real-time correction of accumulated errors for UAV flights in indoor and outdoor environments. We confirmed that our methodology can achieve accumulated error adjustment with the improved relocalization processing in visual odometry. Through our experiments, we confirmed that the distance estimation accuracy was approximately 0.1 (m), and that our methodology can provide smooth flight paths in indoor and outdoor environments.

ACKNOWLEDGMENTS

This research was supported by the METI Monozukuri R&D Support Grant Program for SMEs Grant Number JPJ005698.

REFERENCES

- Mostafa, M., Shady, Z., Adel, M., Naser, E. S. and Abu, S. 2018. Radar and Visual odometry Integrated System Aided Navigation for UAVS in GNSS Denied Environment. *Sensors*, 18(9), pp.13-27.
- Daive, S., Friedrich, F. 2011. Visual odometry[Tutorial]. *IEEE*, 18(4), pp.2-5.
- Faragher, R.M., Harle, R.K. 2013. SmartSLAM - An Efficient Smartphone Indoor Positioning System Exploiting Machine Learning and Opportunistic Sensing. *Nashville*, pp.1006-1019.
- Bassiri, A. et al., 2018. Particle Filter and Finite Impulse Response Filter Fusion and Hector SLAM to Improve the Performance of Robot Positioning. *Journal of Robotics*, pp.5-8.
- Taragay, O., Zhiwei, Z., Supun, S., Rakesh, K. 2007. Visual odometry System Using Multiple Stereo Cameras and Inertial Measurement Unit. *IEEE*, pp.4-8
- Yunliang, J., Yunxi, X., Yong, L. 2013. Performance evaluation of feature detection and matching in stereo visual odometry. *Neurocomputing*, 120, pp.6-10.
- Peidong, L., Marcel, G., Lionel, H., Torsten, S., Andreas, G. and Marc, P. 2018. Towards Robust Visual odometry with a Multi-Camera System. *IEEE*, pp.5-8.